

# DNA nanomachines and nanostructures involving quadruplexes†

Patrizia Alberti, Anne Bourdoncle, Barbara Saccà,‡ Laurent Lacroix and Jean-Louis Mergny\*

Received 21st April 2006

First published as an Advance Article on the web 22nd June 2006

DOI: 10.1039/b605739j

DNA is an attractive component for molecular recognition, because of its self-assembly properties. Its three-dimensional structure can differ markedly from the classical double helix. For example, DNA or RNA strands carrying guanine or cytosine stretches associate into four-stranded structures called G-quadruplexes or i-DNA, respectively. Since 2002, several groups have described nanomachines that take advantage of this structural polymorphism. We first introduce the unusual structures that are involved in these devices (*i.e.*, i-DNA and G-quadruplexes) and then describe the opening and closing steps that allow cycling. A quadruplex–duplex molecular machine is then presented in detail, together with the rules that govern its formation, its opening/closing kinetics and the various technical and physico-chemical parameters that play a role in the efficiency of this device. Finally, we review the few examples of nanostructures that involve quadruplexes.

## Introduction

Although protein machines are abundant, DNA is an attractive component for molecular recognition, because of its self-assembly properties.<sup>1,2</sup> Its pairing specificity and conformational flexibility offer important advantages for the rational design of DNA-based nanostructures, nanomachines or computers. Most of these

*Laboratoire de Biophysique, Muséum National d'Histoire Naturelle USM503, INSERM U565, CNRS UMR 5153, 43 rue Cuvier, 75231, Paris cedex 05, (France). E-mail: faucon@mmhn.fr; Fax: +33-1 40 79 37 05; Tel: +33-1 40 79 36 89*

† This paper was published as part of a themed issue on DNA-based nanoarchitectures and nanomachines.

‡ Current address: Fachbereich Chemie, Biologisch-Chemische Mikrostrukturtechnik, Universität Dortmund, Otto-Hahn-Str. 6, D-44227 Dortmund (Germany).

*Jean-Louis Mergny (born 1966) is currently “Directeur de Recherche” in the INSERM. He received his PhD in 1991. He currently leads a group in the Laboratoire de Biophysique, in the Muséum National d'Histoire Naturelle in Paris, France. He is interested in DNA structure, drug–DNA interactions, telomeres and anticancer drugs.*



Jean-Louis Mergny

devices involve double-stranded DNA. However, DNA “comes in many forms”:<sup>3</sup> its three-dimensional structure can differ markedly from the classical double helix and involve more than two strands. For example, DNA or RNA strands carrying guanine stretches associate into four-stranded structures called G-quadruplexes (Fig. 1B).<sup>4–8</sup>

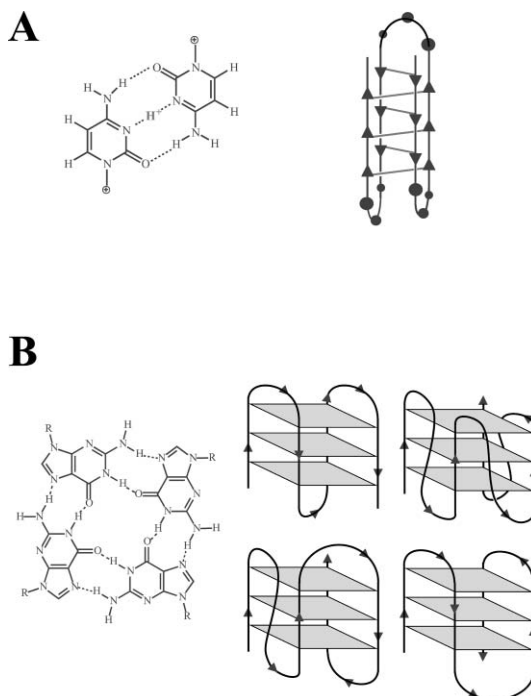


**Fig. 1** Presentation of i-DNA (top) and G-quadruplexes (bottom); (A) C·C<sup>+</sup> base pair (left) and schematic structure of an intramolecular i-DNA (right); (B) a G-quartet (left) and four possible conformations of an intramolecular G-quadruplex (right).

G-quadruplexes are particularly remarkable structures because of their well-defined conformation, their relatively high stability under physiological conditions and high polymorphism. However,

it is only in the past decade that the level of interest in these peculiar structures has increased, due to the hypothesis of a relevant role for G-quadruplex structures in key biological processes and the recent demonstration of their existence *in vivo*.<sup>9–11</sup> Additionally, their capability to form higher order structures such as synapsable DNA or G wires renders these molecules an excellent module for the design of devices for nanotechnology.

In 2002–2003, we<sup>12</sup> and others<sup>13</sup> described a nanomachine that was capable of an extension–contraction movement. This simple and robust device described here is composed of a single 21 base-long oligonucleotide and relies on a duplex/quadruplex equilibrium which may be fuelled by the sequential addition of DNA single-strands, generating a DNA duplex as a by-product. The interconversion between two well-defined topological states induces a two-stroke, linear motor type movement. During the last four years, several improvements have been proposed for this device, and other quadruplex-based machines have been described. Here, we will first present the two unusual structures that are involved in these devices (*i.e.*, i-DNA and G-quadruplexes), and then describe the opening and closing steps that allow cycling. A quadruplex–duplex system will be then presented in detail, together with the rules that govern its formation, its opening/closing kinetics and the various technical and physico-chemical parameters that play a role in the efficiency of this device. Finally, we will present the few examples of nanostructures that involve quadruplex conformations.

## G-quadruplexes

**Presentation.** G-quadruplexes may be formed by intramolecular folding or by association of G-stretches from two or four DNA strands. They result from the hydrophobic stacking of several quartets; each quartet being a planar association of four guanines held together by 8 hydrogen bonds (Fig. 1B, left).<sup>8</sup> A cation (typically Na<sup>+</sup> or K<sup>+</sup>) is located between two quartets forming cation–dipole interactions with eight guanines. This reduces the electronic repulsion of the 2 × 4 central oxygen atoms, thus enhancing hydrogen bond strength and stabilizing quartet stacking. X-Ray crystallography provided definitive evidence of dehydrated cation coordination by G-quartets along the central axis.<sup>14,15</sup> Each quadruplex involving *n* quartets will accommodate (*n* – 1) specific ions. Quadruplex specific stabilization by cations has been evaluated for a long time. Hardin *et al.* defined the following order K<sup>+</sup> > Ca<sup>2+</sup> > Na<sup>+</sup> > Mg<sup>2+</sup> > Li<sup>+</sup> and K<sup>+</sup> > Rb<sup>+</sup> > Cs<sup>+</sup>.<sup>16</sup> A recent study on the human intramolecular telomeric quadruplex determined that Sr<sup>2+</sup> > K<sup>+</sup> > Na<sup>+</sup> ≥ Rb<sup>+</sup> > Li<sup>+</sup> > Cs<sup>+</sup>.<sup>17</sup> The two best-studied ions are Na<sup>+</sup> and K<sup>+</sup>. The preference of quadruplex central cavity for potassium over sodium ions is the result of two opposite effects: from one side the free energy of Na<sup>+</sup> binding to a quadruplex is more favorable than that of K<sup>+</sup>, but from the other side this effect is largely compensated by the much greater cost of Na<sup>+</sup> dehydration.<sup>18,19</sup> The net result is a free energy change in favour of the potassium form.

G-quadruplexes can be classified according to the number of strands that self-associate to form the structure (*i.e.*, one, two or four strands) and further differentiated by the relative orientation of the strands (parallel, anti-parallel or mixed), the orientation of the loops (lateral or diagonal) and the conformation of the guanine bases around the glycosidic bond (*syn* or *anti*).<sup>20</sup> Intramolecular

quadruplexes are often referred to as G<sup>4</sup> DNA. Four guanine blocks must be present on the same oligonucleotide sequence to give rise to the G<sup>4</sup> structure and folding of this oligonucleotide into a quadruplex will create three loops (Fig. 1B, right).

**Kinetics and thermodynamics.** The formation of quadruplex structures, whatever their type may be, is clearly enthalpy driven, with an enthalpy per quartet of –15 to –25 kcal mol<sup>–1</sup>. Overall, the enthalpy per quartet is (unsurprisingly) more negative than the enthalpy per base pair in a double helix.<sup>21</sup> This effect arises from (i) the enthalpic gain of stacking large aromatic surfaces containing polarizable atoms (base stacking itself is driven by electrostatic and van der Waals interactions) and (ii) cation–dipole interactions (see below). This very negative (*i.e.*, favourable) enthalpy is partially compensated by a negative (and unfavourable) entropy of formation. Therefore, G-quadruplex formation shows the classical hallmarks of many nucleic acids structures, with  $\Delta H < 0$  and  $\Delta S < 0$ . Despite the negative contribution of entropy to stability, most quadruplex structures are stable at 37 °C or lower. Another important parameter affecting G-quadruplex formation and conformation is molecular crowding: poly(ethyleneglycol) induces a structural transition from the antiparallel to the parallel G-quadruplex in G<sub>3</sub>T<sub>4</sub>G<sub>4</sub>.<sup>22</sup>

Intramolecular structures (G<sup>4</sup> DNA) fold and unfold (relatively) quickly, and fast mixing experiments (*i.e.*, using a stopped flow accessory) are often required to measure their association and dissociation rates. On the other hand, it is straightforward to obtain equilibrium-melting curves, and this facilitates the determination of thermodynamic parameters (*i.e.*,  $\Delta H^\circ$ ,  $\Delta S^\circ$ ,  $\Delta G^\circ$ , equilibrium constant). These melting curves may be obtained by UV absorbance (at 240 or 295 nm), circular dichroism or fluorescence, once a fluorescent reporter group is attached to the oligomer. One should not forget that this fluorescent group can alter the thermodynamic and kinetic properties of the quadruplexes.

**Structural polymorphism.** Most quadruplexes rely on the formation of a single building block, the G-quartet. Despite a single building block, they present different conformations, depending on the sequence, strand concentration and ionic conditions. Four guanine blocks must be present on the same oligonucleotide sequence and folding of this oligonucleotide into a quadruplex will create three loops. However, variation in the loop geometry and strand orientation may lead to distinct conformations. Several distinct conformations have often been reported for a single guanine-rich sequence, depending on the incubation conditions and the experimental approach (Fig. 1B, right). Such polymorphism complicates the kinetic and thermodynamic analyses of such structures and makes difficult a “clean” design of G<sup>4</sup>-based nanodevices. The most striking and recent example of structural complexity is the intramolecular human telomeric motif. In sodium, the AG<sub>3</sub>(T<sub>2</sub>AG<sub>3</sub>)<sub>3</sub> sequence adopts an intramolecular quadruplex with a central diagonal loop. As a result, each strand has one parallel and one antiparallel neighbour.<sup>23</sup> In potassium, the situation is different. Crystallographic studies indicate that the very same sequence adopts a completely different folding scheme: all four DNA strands are parallel, with the three linking trinucleotide loops positioned on the exterior of the quadruplex core, in a propeller-like arrangement.<sup>24,25</sup> Recent NMR studies by the groups of Yang<sup>26</sup> and Patel demonstrated that the solution conformation in K<sup>+</sup> corresponds to a “mixed” quadruplex, involving one reversal

**Table 1** Comparison of G-quadruplex and i-DNA

Structure	H-bonds <sup>a</sup>	Ion <sup>b</sup>	Sugar <sup>c</sup>	Base <sup>d</sup>	Rise/Å	Twist (deg)	$\Delta H^\circ$ /kcal mol <sup>-1</sup> per quartet or C-C <sup>+</sup> base pair
i-motif	3	H <sup>+</sup>	C3' endo	<i>anti</i>	6.2	16	-11
G-quartet:	4 × 2	K <sup>+</sup> ; Na <sup>+</sup>	C2' endo	<i>syn/anti</i>	3.4	30	-20

<sup>a</sup> Number of H-bonds per repetitive unit (base pair or quartet). <sup>b</sup> Preferred counter-ion. <sup>c</sup> Conformation of the sugar (predominantly observed). <sup>d</sup> Conformation of the glycosidic bond.

chain and two lateral loops. Such polymorphism may explain why complex kinetic behaviours are observed in situations where simpler models are expected.

## i-DNA

**Presentation.** A cytidine-rich oligomer forms a radically different DNA quadruplex in which two parallel duplexes associate in a head-to-tail orientation with their C-C<sup>+</sup> pairs face-to-face, intercalated in a so called i-motif (Fig. 1A).<sup>27</sup> Contrary to the G-quadruplex form, the i-DNA four-stranded structure is not based on quartet formation, but on simple base pairs (Fig. 1A, left and Table 1); therefore, i-DNA is rather a double-duplex than a true quadruplex. i-DNA was the first nucleic acid structure to be elucidated by NMR. Since then, further NMR and X-ray investigations have described the i-motif structure of several C-rich DNA oligomers, including sequences of biological relevance such as the human cytosine rich telomeric repeat.<sup>28</sup> Each intercalated duplex of the i-motif forms a right-handed helix with a helical twist of about 16°. The stacked C-C<sup>+</sup> pairs are nearly orthogonal and the structure has two wide and two very narrow grooves. The intercalation stretches the sugar backbone to an inter-base helical rise of 6.2 Å, about twice that of B-DNA duplexes, and forces the sugar pucker toward the C3'-endo to C4'-exo conformational range.

**Stability.** The optimal pH value for the i-motif stability is equal to the cytidine pK<sub>a</sub> (around 4.2); i-motif formation is disfavoured at basic and very acid pH. The net release of one proton per base pair accounts for the cooperative melting at pH higher than the cytidine pK<sub>a</sub>. Proton release/uptake may be so high that the i-motif structure may be used as a proton donor/acceptor.<sup>29</sup> The telomeric repeat (CCCTAA)<sub>4</sub> can form the i-motif; its half-dissociation temperature (*T*<sub>m</sub>) is 39 °C at pH 6 but is only 20 °C at neutral pH.<sup>30</sup>

## Defining the states of the device

The nanomachines presented here can be compared to two-stroke engines. Various classes of devices are presented in Table 2. In order to characterize the mechanical work associated with an engine cycle, the end-to-end distance variation need to be known. Therefore we shall consider the end-to-end distance in each state of the different motors.

**Table 2** Possible nanodevices

Closed state	Open state	Fuel	Waste	Reference(s)
G-quadruplex	Duplex	Bp formation	Duplex	12,13,32,75
i-DNA duplex	Duplex	pH change	NaCl	44,47
i-DNA	Random coil	pH change	NaCl	45

**The closed/compact state.** For the i-motif based motor, the distance between the first C5' and the last C3' of the sequence is around 0.8 nm. In the G-quadruplex-based motor, use of the same anchor for the first and the last G in the vertebrate telomeric sequence gives rise to a distance in the 1–2 nm range (depending on quadruplex conformation—see Fig. 1B).

**The open/extended state.** For the open state, one may distinguish two different cases. In the case of simple unfolding, the ill-defined open state corresponds to a 21 nucleotide-long single-strand, which should create an object with a maximal length of around 15 nm (fully extended single-strand). However, the actual length is probably much shorter as one should rather consider this object as random coil: single-stranded DNA has a very short persistence length. For the duplex open state, the 5'–3' distance resulting from the unfolding of a 21 nucleotide-long probe is 7.1 nm (using a 0.34 nm pitch).

## Fuelling the device

The flexibility and complementary nature of DNA structures can be used for the fabrication of dynamic assemblies. Cycling oscillation between a folded compact form and an extended motif may be used to perform mechanical work and can be achieved by at least two different pathways: (i) strand replacement, by means of which, distinct base pairing can be switched by the addition of thermodynamically more favourable binding partners (Fig. 3B), and (ii) conformational changes of the nucleic acid molecule as a consequence of environmental modifications (see Table 2; Fig. 3A).

**(a) Via duplex formation (strand displacement).** Conformational changes can be driven by the sequential addition of DNA single strands: the quadruplex sequences (the core of the device) is extended into a duplex structure upon hybridization with a complementary fuel strand (Fig. 2, 3B and 4A); this strand is then displaced by a strand exchange reaction with a second fuel strand, permitting the core sequence to refold into a quadruplex structure. A double-stranded waste product accumulates at each cycle. This approach will be further discussed in more detail. Hybridization kinetics can be controlled by DNA catalysts.<sup>31,32</sup> This “fuelling” principle has been successfully applied for the construction of G4-based mechanical devices, where the transition between a G-quadruplex and a duplex conformation induces extension and contraction of the DNA molecule.<sup>12,13,33</sup> Simmel and co-workers employed this method in an important step towards a real-world application. They opened and closed a G-quadruplex-shaped thrombin-binding aptamer<sup>34</sup> by strand replacement, allowing the release or binding of a thrombin molecule in the presence of a specific DNA sequence.<sup>33</sup>

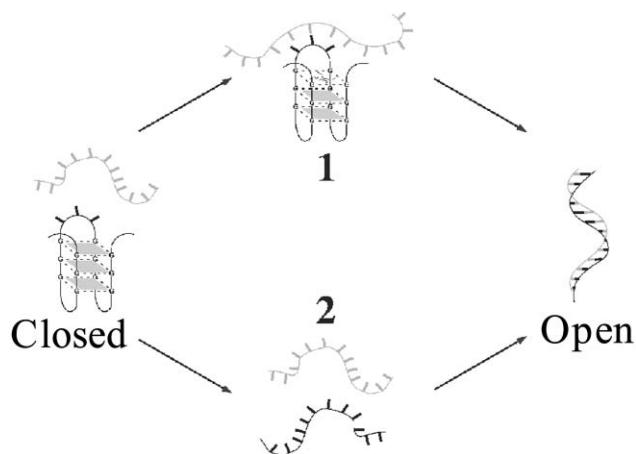


**Fig. 2** Opening of the G-quadruplex; two possible pathways are presented. Upper: *via* direct binding to the folded quadruplex, followed by duplex invasion. This mechanism is considered unlikely if loops are short; however, a variation of this pathway in which the quadruplex is only partially unfolded is possible. Lower: *via* trapping the open state of the quadruplex. If one chooses experimental conditions too favourable for quadruplex formation, extremely slow kinetics are expected, as a result of a long-lived folded state.

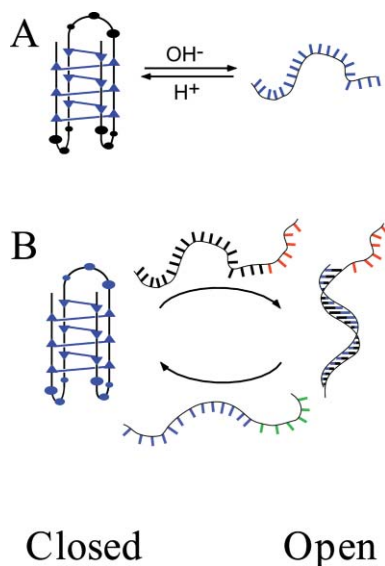


**Fig. 3** Two possible nanodevices involving i-DNA (A) pH-driven: a proton fuelled nanodevice consisting of a C-strand capable of folding in an i-motif.<sup>34</sup> At low pH, folding of the C-strand into an i-motif is favoured (left). Raising the pH destabilises the i-motif, thus promoting an extended single-stranded state (right) or duplex conversion (provided a complementary strand is present, as panel B). (B) Addition of the red/black strand leads to the opening of the closed state (upper pathway). The blue/green strand hybridizes to the black/red strand, which releases the blue strand that folds back into the closed state (lower pathway).

Most of the DNA devices involving quadruplexes rely on duplex–quadruplex interconversion, which has been studied for a number of different sequences.<sup>16,35–39</sup> In particular, an equimolar mixture of the telomeric oligonucleotides  $AG_3(TTAG_3)_3$  and  $(C_3TAA)_3C_3T$ , has been the subject of our investigations. We defined which structures exist in solution and which are the predominant species under a variety of experimental conditions.<sup>40</sup>

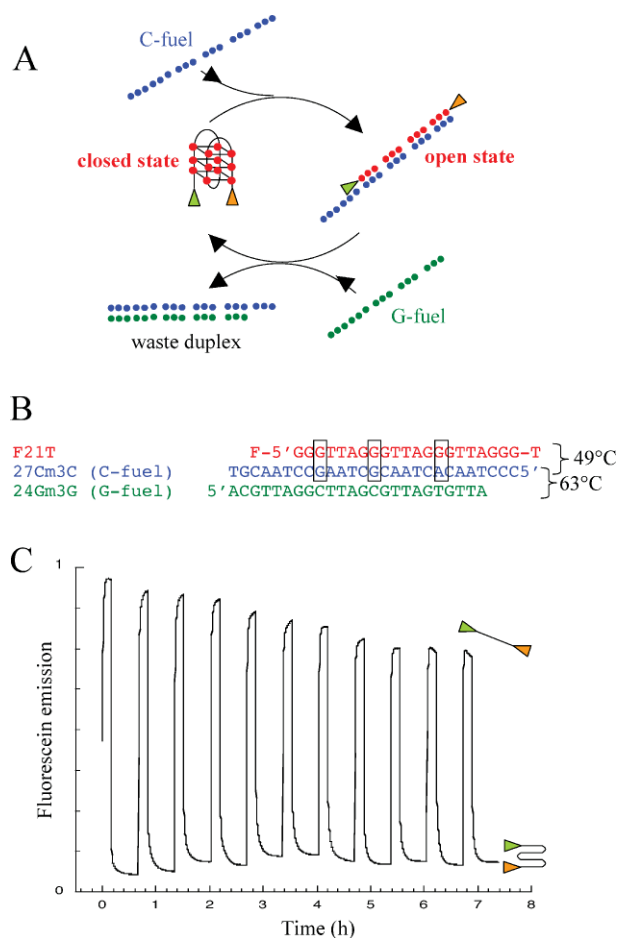


**Fig. 4** A DNA-fuelled nanodevice involving a G-quadruplex. (A) Principle of the device: F21T is folded into a quadruplex structure. In the opening step, the addition of a complementary strand (C-fuel) extends F21T into a duplex conformation. In the closing step, the C-fuel is removed from F21T by the addition of a complementary G-fuel and F21T refolds in a quadruplex form. A waste duplex is generated at each cycle. (B) Sequence of the oligomers. The  $T_m$  of the two duplexes F21T–C-fuel and C-fuel–G-fuel are shown on the right. They were obtained in a 10 mM sodium cacodylate pH 7.2 buffer with 0.1 M NaCl at a strand concentration of 2  $\mu$ M (for F21T) and 2.5  $\mu$ M (C-fuel–G-fuel). The addition of 20 mM  $MgCl_2$  leads to a  $T_m$  increase of 5–8  $^{\circ}C$ . Mismatches between F21T and the C-fuel 27Cm3C are boxed. (C) Cycling of the device in a 10 mM sodium cacodylate pH 7.2 buffer with 0.1 M KCl and 20 mM  $MgCl_2$ , at 45  $^{\circ}C$ . The concentrations of F21T and of the fuel strands are 2 and 2.5  $\mu$ M, respectively. F21T conformational oscillations are monitored by FRET between a fluorescein (F, green triangle) and a tetramethylrhodamine (T, orange triangle).

Under near-physiological conditions of pH, temperature and salt concentration, telomeric DNA is predominantly in a double-helical form. However, at lower pH values, favourable ionic conditions or higher temperatures, the G-quadruplex and/or the i-motif efficiently compete with the duplex.<sup>39,40</sup> We then demonstrated that, in the  $\mu$ M range, the duplex is the thermodynamically favoured species and that folding into a quadruplex delays, but does not prevent, formation of a Watson–Crick duplex.<sup>12,41</sup> The increased stability of the duplex as compared to the quadruplex has been confirmed by UV-melting analysis of the oligonucleotides under a variety of conditions. For example, the  $\Delta G^{\circ}$  for quadruplex formation at 37  $^{\circ}C$  in 0.1 M KCl is  $-3.8$  kcal mol<sup>-1</sup> for

the intramolecular telomeric sequence, and the  $\Delta G^\circ$  for duplex formation under identical conditions is significantly more negative ( $< -5 \text{ kcal mol}^{-1}$ ). Invasion of the thrombin-binding quadruplex by a complementary DNA strand fails, whereas a short PNA probe actively disrupts the quadruplex.<sup>36</sup>

These results suggest that human telomeric quadruplexes are marginally less stable than duplexes. In the absence of external factors, such as supercoiling or structure-specific binding proteins, a genomic region with strong asymmetry between a guanine-rich and a cytosine-rich strand is likely to remain double-stranded. However, the situation in a living cell is inherently molecularly-crowded. This molecular crowding affects the structure and stability of the telomeric G-rich and C-rich strands and may prevent any duplex formation.<sup>42</sup> Ciliate telomeric motifs such as  $(G_4T_4)_n$  (*Oxytricha*) prefer quadruplexes over duplexes under certain conditions. The  $G_4T_4G_4$  sequence forms a duplex in the presence of its complementary strand in 150 mM  $\text{Na}^+$ , but retains a quadruplex conformation in  $\text{K}^+$ .<sup>35</sup> Higher sodium concentrations ( $> 550 \text{ mM}$ ) are required to induce duplex disproportionation.

Analysis of duplex formation/quadruplex opening is further complicated by the existence of several possible quadruplex conformations (Fig. 1B) and several possible pathways (Fig. 2). This might explain the necessity of a double-exponential fit to investigate the results.<sup>43</sup> The first-order kinetics observed by Green *et al.* suggest a slow rearrangement of the quadruplex prior to trapping. Finally, one should note that the double-labelling fluorophore procedure leads to a  $10^\circ\text{C}$  decrease in melting temperature and we do not know whether this reflects a decrease in association and/or an increase in dissociation as compared to the unlabelled  $(G_3T_2A)_3G_3$  quadruplex. This labelling could also favour some folded forms and therefore alter the opening/folding pathways.

**(b) By changing the medium.** A second approach to obtain DNA-based nanomachines relies on environmentally-induced conformational changes. Such external factors include the variation of salt concentrations that control supercoiling, ionic strength, pH value and temperature. All these structural changes are reversible and, hence, the direction of the transition can be inverted by oscillating the value of the environmental parameter. Two examples illustrating this principle have been recently reported by the groups of S. Balasubramanian and F. Simmel<sup>44,45</sup> (Fig. 3). They used protons to fuel a DNA-based nanomachine which can reversibly switch between an i-motif conformation (compact, closed state) and an extended conformation, either a random coil or a double-stranded structure. pH oscillations may be generated by sequential addition of HCl and NaOH, leading to the accumulation of NaCl and  $\text{H}_2\text{O}$  as waste products, or by sophisticated oscillatory chemical reactions. In the case of pH driven nanodevices, it is essential to choose a probe which is relatively insensitive to pH. Rhodamine green is an excellent choice, as its quantum yield is insensitive to pH from 4 to 9.

### Immobilized devices

Most artificial DNA devices work in buffer solution and thus produce nondirected random motion. To exploit the potential of these motors, it is necessary to attach them to a surface without altering their function. By immobilizing a DNA nanodevice onto micro-cantilevers, Shu *et al.* demonstrated that it is possible to convert the conformational change of the i-motif into cantilever bending.<sup>46</sup> An

i-motif may also be immobilized on a gold surface; when folded, the terminal rhodamine green fluorophore is quenched due to its close proximity to the gold surface.<sup>47</sup> Increasing the pH allows unfolding of the structure and hybridization to a complementary strand, lifting the fluorophore away from the gold surface, and greatly reducing quenching efficiency. Xiao *et al.*<sup>48</sup> used a similar approach to develop a thrombin detector. They immobilized a thrombin-binding aptamer on a gold electrode and labelled it with methylene blue (MB). In the absence of thrombin, the aptamer is in a conformational equilibrium between the G-quadruplex and the unfolded state such that the MB labels of unfolded aptamers may enable efficient electron transfer with the electrode. The presence of thrombin shifts this equilibrium towards the thrombin-binding G-quadruplex conformation, thus altering the electron tunnelling distance and thus inhibiting electron transfer.

### Illustration of a quadruplex–duplex device

**(a) Description.** In this paragraph, we will present the cycling of a G-quadruplex-based device. The principle and the cycling of the device are illustrated in Fig. 4. We have chosen to study the F21T sequence (see Fig. 4B) that mimics 3.5 repeats of the human telomeric G-strand. This device switches between two states: an elongated double strand of DNA and a tightly coiled quadruplex.<sup>12</sup> Addition of a fuel DNA strand leads to unfolding of the quadruplex structure and consequent formation of a classical double helix. To re-fold the quadruplex, we add an “anti-fuel”, which combines with the DNA fuel strand to form a waste product. The device oscillates between two well-defined states (a folded quadruplex and an extended duplex) and accomplishes an extension–contraction movement.<sup>12</sup> The 5’–3’ distance oscillates between 1.5 nm (quadruplex) and 7 nm (duplex), with a calculated force of *ca.* 8 pN.<sup>12</sup> The presence of two fluorescent reporter groups (fluorescein and tetramethylrhodamine) allows us to monitor the conformational transition between the folded and the unfolded form (Fig. 4C). In fact, as previously reported by our group,<sup>49</sup> intramolecular folding of a telomeric oligonucleotide into an intramolecular G-quadruplex leads to fluorescence resonance energy transfer (FRET) between a donor (fluorescein) and an acceptor (tetramethylrhodamine) covalently attached to the 5’ and 3’ ends of the DNA strand, respectively.

The first step of the machine (the opening step; Fig. 2) consists in opening the quadruplex into a duplex conformation. Conversion of the 21 nucleotide-long intramolecular quadruplex  $d(\text{GGG}(\text{TTAGGG})_3)$  into a double-helix upon addition of the complementary 21C strand is associated to little transfer, as the average distance of the two chromophores is larger than the Förster critical distance (calculated to be around 5.0 nm). In contrast, intramolecular folding brings the two chromophores in sufficiently close proximity to observe energy transfer. Duplex formation does not occur at  $0^\circ\text{C}$ , whereas it is strongly delayed at  $20^\circ\text{C}$  and is almost complete after 1 h at  $37^\circ\text{C}$  or higher. Faster kinetics were observed in the presence of 0.1 M NaCl (instead of KCl).<sup>12</sup> These results indicate that, provided that a suitable temperature is chosen, association between the two strands is possible. This process corresponds to the first half of the cycle depicted in Fig. 4A.

To promote quadruplex opening, a complementary 21 base-long  $d(\text{CCCTAA})_3\text{CCC}$  oligonucleotide (C-fuel) is sufficient. However,

the reversal step requires a longer C-fuel strand length, in order to initiate C-fuel/G-fuel duplex formation on a single-stranded overhang. We therefore analyzed F21T quadruplex opening by longer C-fuel strands, which contain 6 or 12 extra bases at their 3' end (*i.e.*, 27- or 33-mers; Fig. 4B). The presence of a 6–12 base-long overhang does not hamper F21T/C-fuel duplex formation and does not significantly alter the kinetics of quadruplex-to-duplex conversion.

The second step of the machine (the closing step) consists of the reverse equilibrium: opening of the C-fuel/F21T duplex with consequent liberation of the F21T strand, thus allowing for its intramolecular quadruplex refolding. The F21T strand may be liberated with another DNA strand called the G-fuel strand. This strand allows for the destruction of the non-covalent interactions within the C-fuel/F21T duplex by formation of a thermodynamically more stable C-fuel/G-fuel competing duplex.

**(b) Poisoning by the duplex waste product.** The progressive accumulation of the waste duplex will displace the equilibrium toward the extended state and eventually poison the system. We have tried to calculate the influence of this waste product on the equilibrium constant (Fig. 5A).  $K$  is defined as the ratio between the affinity constants of the two duplexes (C-fuel/F21T duplex and C-fuel/G-fuel). As shown in this figure, in the case of equal ( $K = 1$ ) or not sufficiently different ( $K = 10$ ) affinity constants, the cycling efficiency will decrease very quickly after a few cycles, whereas a large difference in affinity ( $K = 10^3$  to  $10^4$ ) allows efficient cycling for 20 times or more. In the latter case, the accumulation of the waste product may be neglected. These calculations are in agreement with the experimental data. In the example of Fig. 5B, the two duplexes F21T/27C and 27C/24G have very similar stabilities: the fast decrease in cycling efficiency is consistent with the simulated data assuming  $K = 1$  (circles) and may simply be

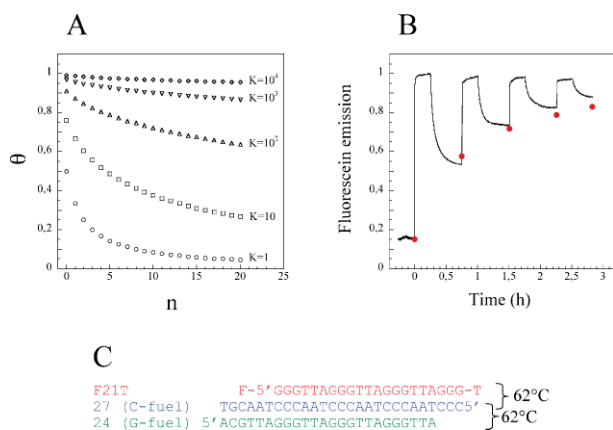


**Fig. 5** Influence of the accumulation of the waste product on the cycling efficiency. (A)  $\theta$  is the fraction of F21T refolded into a G-quadruplex form at the end of each cycle as a function of the number  $n$  of performed cycles. It is related to the equilibrium constant  $K$  between the folded and the extended state at the closing step by the expression  $K = [\theta(n + \theta)/(1 - \theta)^2]$ .  $K$  is defined as  $K = \frac{[(F21T)_{quadruplex}][C-fuel][G-fuel]_{duplex}}{[(F21T/C-fuel)_{duplex}][G-fuel]}$ . (B) Cycling of the core sequence F21T (0.2  $\mu$ M) using the fuels strands 27C and 24G (0.25  $\mu$ M), in a 10 mM sodium cacodylate pH 7.2 buffer with 0.1 M NaCl and 20 mM MgCl<sub>2</sub>, at 37 °C. The filled circles represent the attended signals at the end of each folding step assuming  $K = 1$ . (C) Sequences of the oligomers: the  $T_m$  of the two duplexes F21T/27C and 27C/24G are shown on the right. They were obtained under the same conditions as Fig. 4B.

explained by the accumulation of the 27C/24G waste product. To increase the cycling efficiency of the nanodevice, two solutions are viable: *increasing* the stability of the C-fuel/G-fuel duplex using a modified morpholino G-fuel strand or *decreasing* the stability of the F21T/C-fuel duplex by introducing mismatches (Fig. 4B). Contrary to the system presented in Fig. 5B, both solutions lead to a near complete reversion to the folded quadruplex.<sup>12</sup>

The C-fuel/G-fuel strand ratio must also be precisely controlled. As strand concentrations are usually determined with a 10% or more uncertainty using calculated extinction coefficients, it is necessary to pre-establish molar equivalence between these two strands by preliminary UV-absorbance titration profiles. Otherwise, the accumulation of a slight excess of the C- or G-fuel strand eventually leads to the poisoning of the machine (data not shown).

**(c) Improving the kinetics.** The switching time for this machine may be modulated by a number of factors, such as temperature, nature of the monovalent cation,<sup>12</sup> ionic strength, presence of divalent cations, sequence and chemical modification of the strand(s) as well as the strand concentration. It is important to note that magnesium has a favourable effect on the kinetics of the system, except when a morpholino G-fuel strand is used.<sup>12</sup> Magnesium does not stabilize the DNA–morpholino duplex, perhaps because morpholino oligomers are uncharged nucleic acid analogs.<sup>50</sup> Using strand concentrations in the  $\mu$ M range leads to acceptable kinetics: increasing strand concentrations from 0.2 to 2  $\mu$ M leads to faster opening and closing steps of the nanodevice. From these data, and from the comparison of different oligonucleotide sequences, it is possible to design an experimental system in which the machine has a relatively fast cycle.<sup>12</sup> The pH was kept above 7.0 in all experiments for two reasons: fluorescein emission is strongly quenched at acidic pH and a low pH may favour alternative structures of the C-rich strand.<sup>51,52</sup> Under optimal conditions, switching from the closed to the open state takes less than 30 s, while the reverse process takes 3 s.

## Nanostructures involving quadruplexes

DNA is an excellent molecule not only for design of nanodevices but also for construction of complex two- and three-dimensional DNA nanoarchitectures (for a recent illustration, see<sup>2</sup>). In most cases, “traditional” Watson–Crick base pairing is the fundamental driving force for specific recognition and assembly. However, complex self-assembling building blocks are required for the production of stable nanosized objects or nanoarrays. A pioneering work in this field was conducted by Seeman in the early 1980s:<sup>53</sup> synthetic DNA branched junctions, containing three or four arms, were used as building blocks for the construction of artificial DNA nanostructures. DNA junction motifs are comprised of double-stranded DNA helices where one half of each ssDNA strand contributes to one arm and the other half is linked to a neighbouring arm. This increases the stiffness of the DNA rod, which otherwise, with its persistence length of *ca.* 50 nm, would lead to severe deformations for structures in the  $\mu$ m scale. Additional rigidity may be conferred to the structure by use of the so-called double crossover tiles.<sup>54,55</sup> These motifs consist of two double-stranded DNA helices which interchange their single-strands at two crossover points. A potential alternative would be to use a DNA structure whose formation is not based on

“classical” Watson–Crick base-pairing, such as a quadruplex. NMR, crystallography and molecular modelling studies agree that this structure has an exceptional stiffness.<sup>56</sup>

Guanine-rich oligonucleotides may indeed self assemble into supermolecular structures called G-wires<sup>57</sup> or frayed-wires.<sup>58</sup> G-wires formed by  $G_4T_2G_4$ <sup>57</sup> are up to 1  $\mu\text{m}$  long, with a diameter (2.5 nm) consistent with the diameter of the G-quadruplex. Formation of G-wires is dependent on the presence of  $\text{Na}^+$ ,  $\text{K}^+$  and/or  $\text{Mg}^{2+}$  and, once formed, G-wires are resistant to denaturation. Assembly of  $G_4T_2G_4$  G-wires occurs more efficiently in  $\text{Na}^+$ , yet G-wires formed in potassium are more stable.<sup>57</sup> Several reports indicate the crucial role played by divalent cations such as magnesium<sup>59–61</sup> or calcium<sup>62</sup> on G-wire formation.  $\text{Ca}^{2+}$  induces a structural transition of the  $G_4T_4G_4$  oligonucleotide from the antiparallel to the parallel G-quadruplex, and finally to G-wire formation.<sup>62</sup> The kinetic parameters also indicate that  $G_4T_4G_4$  undergoes this transition through multiple steps involving  $\text{Ca}^{2+}$  binding, isomerization and oligomerization of  $G_4T_4G_4$ . These complexes form within minutes<sup>58</sup> or hours, even at moderate concentrations. In the case of the  $A_{15}G_{15}$  oligonucleotide, a “stem” is formed through interactions between the guanine residues of the associated oligonucleotides, whereas the adenine “arms” remain single-stranded and may be hybridized to a  $T_{10}$  or  $T_{15}$  oligomer without disrupting the quadruplex stem.<sup>58,59</sup> An interesting (but speculative) new model for multimerization called “G-lego” has recently been proposed for  $G_{11}T$ .<sup>63</sup> This model requires the rearrangement and sharing of hydrogen bonds to form a new quartet between two interacting quartets. Once formed, all these complexes are extremely resistant. G-wires prepared in the presence of potassium resist even to standard denaturation conditions (40–50% formamide/7–8 M urea 100 °C).<sup>57,58</sup>

Unfortunately, G-wires are relatively “crude” supramolecular assemblies: although the formation of  $\mu\text{m}$  long rods is straightforward, it is difficult to control precisely the assembly process and to combine these wires with more complex motifs. Frayed wires bearing additional dangling ends at each building block were employed to construct networks using linker strands that form Watson–Crick and Hoogsteen base pairs with the “fringes”. These assemblies were characterized by AFM.<sup>64</sup> The assembly of branched nanowires of guanine quadruplexes has also been demonstrated.<sup>65</sup>

Short, well-defined tetramolecular quadruplexes have not yet been used for the construction of self-assembling DNA nanoarchitectures because of their self-pairing properties (in a G4 structure, G binds to G: the concept of *complementary* strand does not apply here). If such a motif can hardly qualify as the basis for well-defined, complex nanostructures, it can still be part of a duplex-based architecture. Liu *et al.* introduced a G-quadruplex aptamer in a DNA nanostructure to drive the self assembly of the thrombin polypeptide.<sup>66</sup>

## Discussion and concluding remarks

Although nanotechnology is “trendy”, everything with the prefix “nano” is not necessarily novel: a number of biological macromolecules undergo conformational changes or reactions that are potentially reversible and fuelled by environmental stimuli ( $\text{H}^+$ , small molecules, *etc.*—a beautiful example is provided by ATP synthase). These biomolecules may therefore be described

as nanomachines. Clearly, to re-label these existing systems as nanomachines, without either gaining deeper understanding about how they work or finding new applications, is not in itself inventive. One may for example consider a triplex–duplex conversion: this system, which has been studied before in great detail,<sup>67–69</sup> may be assimilated to a proton-fuelled nanomachine if the third strand is tethered to the duplex.<sup>70</sup> In the same line, the discovery of guanine quartets represented an important step forward in our understanding of DNA structure.<sup>4–6,71,72</sup> On the other hand, practical applications of quadruplex-based nanodevices are yet to be demonstrated; we will discuss some possibilities in the next paragraph.

Potential applications of quadruplex-based nanoarchitectures include from one side the use of more rigid DNA scaffolds for the precise positioning of macromolecules (at the nanometer scale) whereas, from the other side, the controlled conformational transition from the folded quadruplex to the extended duplex form may be employed in the field of nanorobotics. Quadruplex structures comprise a wide class of well-defined conformational states. Their conformation and stability can be tuned by varying the sequence and/or the length sequences, by modifying different solution conditions, such as salt composition or pH, or by using small molecules that specifically bind to them. Although our understanding of the thermodynamic, kinetic and structural properties of quadruplexes has improved, considerable work lies ahead to fully understand the rules governing their formation, in order to design new devices and architectures involving quadruplexes. A deeper comprehension of these rules will permit the exploitation of the structural richness offered by quadruplexes and the control and modulation of the characteristics defining quadruplex based devices, such as the conformational states, the nature and the amplitude of the performed movements, the forces that may be exerted and their robustness. A weakness of DNA-fuelled nanodevices is their oscillation frequency, limited by the hybridization kinetics of complementary strands. DNA catalysts may be designed to speed up cycling as it has been recently demonstrated.<sup>53</sup> Another potential limitation of quadruplex based nanomachines at least as they are conceived up to now is the need for sequential addition of fuel (protons or DNA-strands) to make them cycling. It will be interesting to conceive systems capable of cycling autonomously, as recently reported for “walking DNA”.<sup>73</sup> Furthermore, accumulation of waste products (DNA or salt) leads to a progressive loss of cycling efficiency, as we have shown for DNA-fuelled nanodevices. The progressive increase in salt concentration in the proton fuelled device represented in Fig. 3A should also lead to a slow oscillation damping by stabilizing the duplex over the i-motif. In order to make a device run indefinitely, the parameters governing quadruplex–duplex equilibrium should be kept constant, but this can occur, of course, only at the expense of some external system.

A still open question concerns the closing and opening pathways of DNA nanodevices based on quadruplex/duplex interconversion (and more generally, DNA-fuelled nanodevices). Is the opening step driven by a strand exchange reaction (pathway 1, Fig. 2) or is it driven by an equilibrium displacement induced by hybridization of the complementary strand with an unfolded core sequence (pathway 2, Fig. 2)? The change in free energy between the closed and the open state does not depend on the opening pathway, the free energy being a state function. On the other hand,

the work that can be accomplished by the system depends on the pathway experienced (that is, on the kind of forces applied to the system which may affect the dissipation of energy). The same question may be addressed for the closing step.

A legitimate question is: what are these devices good for? The first pioneering works describing DNA nanodevices principally anticipated potential applications in the field of nanorobotics. These devices permit a wide range of movements at the nanometer scale. They are, in principle, capable of exerting forces comparable to those exerted by natural molecular motors (in the order of 10 pN). They switch between well-defined conformational states, thus offering the possibility to code different information. Can these systems also be exploited for biological applications? A partial answer may be found in a communication by Dittmer *et al.*<sup>33</sup> this team used a DNA-fuelled system based on quadruplex–duplex transition (similar to the one represented in Fig. 4A) to control the concentration of the human blood-clotting  $\alpha$ -thrombin in solution. The core sequence is an aptamer that, when folded in a quadruplex structure, strongly binds to thrombin; switching between a quadruplex and a duplex conformation leads to trapping and releasing of thrombin, respectively. May this approach be extended to regulate other biological processes, for example, to modulate biological processes occurring at DNA or RNA level? Sequences prone to form quadruplexes are present in the regulatory regions of genomes and it has been suggested that the transitory formation of quadruplex structures may play a role in genome regulation. For example, Hurley and colleagues reported that the stabilization of a G-quadruplex structure in the c-MYC promoter region by a small molecule repressed transcription.<sup>74</sup> Starting from a duplex conformation, is it possible to enforce artificially duplex–quadruplex conversion in certain genome or RNA regions by using fuel oligonucleotides, following the principle illustrated in Fig. 4A?

Finally, as Richard Feynman said at the annual meeting of the American Physical Society in 1959 in a visionary talk entitled “There is plenty of room at the bottom”: “... (W)hat are the possibilities of small but movable machines? They may or may not be useful, but they surely would be fun to make.”

## Acknowledgements

We thank C. Gosse (Marcoussis, France) for helpful discussions and the referees for their suggestions. This work was supported by ARC (# 3365 to J.L.M.) and E.U. FP6 “MolCancerMed” (LSHC-CT-2004-502943) grants.

## References

- 1 C. M. Niemeyer and M. Adler, *Angew. Chem., Int. Ed.*, 2002, **41**(20), 3779–3783.
- 2 P. W. Rothemund, *Nature*, 2006, **440**(7082), 297–302.
- 3 A. Rich, *Gene*, 1993, **135**(1–2), 99–109.
- 4 E. Henderson, C. C. Hardin, S. K. Walk, I. Tinoco, Jr. and E. H. Blackburn, *Cell*, 1987, **51**, 899–908.
- 5 W. I. Sundquist and A. Klug, *Nature*, 1989, **342**, 825–829.
- 6 J. R. Williamson, M. K. Raghuraman and T. R. Cech, *Cell*, 1989, **59**, 871–880.
- 7 R. Jin, K. J. Breslauer, R. A. Jones and B. L. Gaffney, *Science*, 1990, **250**, 543–546.
- 8 J. R. Williamson, *Annu. Rev. Biophys. Biomol. Struct.*, 1994, **23**, 703–730.

- 9 C. Schaffitzel, I. Berger, J. Postberg, J. Hanes, H. J. Lipps and A. Plückthun, *Proc. Natl. Acad. Sci. U. S. A.*, 2001, **98**, 8572–8577.
- 10 M. L. Duquette, P. Handa, J. A. Vincent, A. F. Taylor and N. Maizels, *Genes Dev.*, 2004, **18**(13), 1618–1629.
- 11 K. Paeschke, T. Simonsson, J. Postberg, D. Rhodes and H. Lipps, *Nat. Struct. Mol. Biol.*, 2005, **12**(10), 847–854.
- 12 P. Alberti and J. L. Mergny, *Proc. Natl. Acad. Sci. U. S. A.*, 2003, **100**(4), 1569–1573.
- 13 J. J. Li and W. Tan, *Nano Lett.*, 2002, **2**(4), 315–318.
- 14 G. Laughlan, A. I. H. Murchie, D. G. Norman, M. H. Moore, P. C. E. Moody, D. M. J. Lilley and B. Luisi, *Science*, 1994, **265**(5171), 520–524.
- 15 K. Phillips, Z. Dauter, A. I. H. Murchie, D. M. J. Lilley and B. Luisi, *J. Mol. Biol.*, 1997, **273**(1), 171–182.
- 16 C. C. Hardin, T. Watson, M. Corregan and C. Bailey, *Biochemistry*, 1992, **31**(3), 833–841.
- 17 A. Włodarczyk, P. Grzybowski, A. Patkowski and A. Dobek, *J. Phys. Chem. B*, 2005, **109**, 3594–3605.
- 18 N. V. Hud, F. W. Smith, F. A. L. Anet and J. Feigon, *Biochemistry*, 1996, **35**(48), 15383–15390.
- 19 J. Gu and J. Leczczyński, *J. Phys. Chem. A*, 2002, **106**, 529–532.
- 20 M. A. Keniry, *Biopolymers*, 2001, **56**(3), 123–146.
- 21 D. S. Pilch, G. E. Plum and K. J. Breslauer, *Curr. Opin. Struct. Biol.*, 1995, **5**(3), 334–342.
- 22 D. Miyoshi, A. Nakao and N. Sugimoto, *Biochemistry*, 2002, **41**, 15017–15024.
- 23 Y. Wang and D. J. Patel, *Structure*, 1993, **1**(4), 263–282.
- 24 G. N. Parkinson, M. P. H. Lee and S. Neidle, *Nature*, 2002, **417**, 876–880.
- 25 S. Neidle and G. N. Parkinson, *Curr. Opin. Struct. Biol.*, 2003, **13**(3), 275–283.
- 26 A. Ambrus, D. Chen, J. Dai, T. Bialis, R. A. Jones and D. Yang, *Nucleic Acids Res.*, 2006, **34**(9), 2723–2735.
- 27 K. Gehring, J. L. Leroy and M. Guéron, *Nature*, 1993, **363**, 561–565.
- 28 A. T. Phan and J. L. Leroy, *J. Biomol. Struct. Dyn.*, 2002, **S2**, 245–252.
- 29 J. Völker, H. H. Klump and K. J. Breslauer, *Proc. Natl. Acad. Sci. U. S. A.*, 2001, **98**(14), 7694–7699.
- 30 J. L. Leroy, M. Guéron, J. L. Mergny and C. Hélène, *Nucleic Acids Res.*, 1994, **22**(9), 1600–1606.
- 31 A. J. Tuberfield, J. C. Mitchell, B. Yurke, A. P. Mills, M. I. Blakey and F. C. Simmel, *Phys. Rev. Lett.*, 2003, **90**(11), 118102–118104.
- 32 Y. Wang, Y. Zhang and N. P. Ong, *Phys. Rev. E*, 2005, **72**, 0521918.
- 33 W. U. Dittmer, A. Reuter and F. C. Simmel, *Angew. Chem., Int. Ed.*, 2004, **43**(27), 3550–3553.
- 34 R. F. Macaya, P. Schultze, F. W. Smith, J. A. Roe and J. Feigon, *Proc. Natl. Acad. Sci. U. S. A.*, 1993, **90**(8), 3745–3749.
- 35 T. Miura and G. J. Thomas, *Biochemistry*, 1994, **33**(25), 7848–7856.
- 36 B. Datta and B. A. Armitage, *J. Am. Chem. Soc.*, 2001, **123**(39), 9612–9619.
- 37 H. Deng and W. H. Braunlin, *Biopolymers*, 1995, **35**(6), 677–681.
- 38 M. Salazar, B. D. Thompson, S. M. Kerwin and L. H. Hurley, *Biochemistry*, 1996, **35**(50), 16110–16115.
- 39 W. Li, P. Wu, T. Ohmichi and N. Sugimoto, *FEBS Lett.*, 2002, **526**(1–3), 77–81.
- 40 A. T. Phan and J. L. Mergny, *Nucleic Acids Res.*, 2002, **30**(21), 4618–4625.
- 41 P. Alberti and J. L. Mergny, *Cell. Mol. Biol.*, 2004, **50**(3), 241–253.
- 42 D. Miyoshi, S. Matsumura, S. Nakano and N. Sugimoto, *J. Am. Chem. Soc.*, 2004, **126**(1), 165–169.
- 43 J. J. Green, L. M. Ying, D. Klenerman and S. Balasubramanian, *J. Am. Chem. Soc.*, 2003, **125**(13), 3763–3767.
- 44 D. Liu and S. Balasubramanian, *Angew. Chem., Int. Ed.*, 2003, **42**, 5734–5736.
- 45 T. Liedl and F. C. Simmel, *Nano Lett.*, 2005, **5**(10), 1894–1898.
- 46 W. Shu, D. Liu, M. Watari, C. K. Riemer, T. Strunz, M. E. Welland, S. Balasubramanian and R. A. McKendry, *J. Am. Chem. Soc.*, 2005, **127**(48), 17054–17060.
- 47 D. Liu, A. Bruckbauer, C. Abell, S. Balasubramanian, D.-J. Kang, D. Klenerman and D. Y. Zhou, *J. Am. Chem. Soc.*, 2006, **128**, 2067–2071.
- 48 Y. Xiao, A. A. Lubin, A. J. Heeger and K. W. Plaxco, *Angew. Chem., Int. Ed.*, 2005, **44**(34), 5456–5459.
- 49 J. L. Mergny and J. C. Maurizot, *ChemBioChem*, 2001, **2**, 124–132.
- 50 J. Summerton and D. Weller, *Antisense Nucleic Acid Drug Dev.*, 1997, **7**, 187–195.
- 51 J. L. Mergny, L. Lacroix, X. Han, J. L. Leroy and C. Hélène, *J. Am. Chem. Soc.*, 1995, **117**(35), 8887–8898.



- 
- 52 J. L. Mergny, *Biochemistry*, 1999, **38**, 1573–1581.  
53 N. C. Seeman, *J. Theor. Biol.*, 1982, **99**(2), 237–247.  
54 T. J. Fu and N. C. Seeman, *Biochemistry*, 1993, **32**(13), 3211–3220.  
55 P. Sa-Ardyen, A. V. Vologodskii and N. C. Seeman, *Biophys. J.*, 2003, **84**(6), 3829–3837.  
56 R. Stefl, N. Spackova, I. Berger, J. Koca and J. Sponer, *Biophys. J.*, 2001, **80**(1), 455–468.  
57 T. C. Marsh and E. Henderson, *Biochemistry*, 1994, **33**(35), 10718–10724.  
58 E. Protozanova and R. B. Macgregor, *Biochemistry*, 1996, **35**(51), 16638–16645.  
59 E. Protozanova and R. B. Mac Gregor, *Biophys. J.*, 1998, **75**(2), 982–989.  
60 E. Protozanova and R. B. Mac Gregor, *Biophys. Chem.*, 2000, **84**, 137–147.  
61 S. P. Marotta, P. A. Tamburri and R. D. Sheardy, *Biochemistry*, 1996, **35**(32), 10484–10492.  
62 D. Miyoshi, A. Nakao and N. Sugimoto, *Nucleic Acids Res.*, 2003, **31**(4), 1156–1163.  
63 M. Biyani and K. Nishigaki, *Gene*, 2005, **364**, 130–138.  
64 M. A. Batalia, E. Protozanova, R. B. MacGregor, Jr. and D. A. Erie, *Nano Lett.*, 2002, **2**(4), 269–274.  
65 C. Zhou, Z. Tan, C. Wang, Z. Wei, Z. Wang, C. Bai, J. Qin and E. Cao, *J. Biomol. Struct. Dyn.*, 2001, **19**, 807–812.  
66 Y. Liu, C. Lin, H. Li and H. Yan, *Angew. Chem., Int. Ed.*, 2005, **44**(28), 4333–4338.  
67 H. E. Moser and P. B. Dervan, *Science*, 1987, **238**, 645–650.  
68 T. Le Doan, L. Perrouault, M. Chassignol, N. T. Thuong and C. Hélène, *Nucleic Acids Res.*, 1987, **15**, 8643–8659.  
69 J. Völker, D. P. Botes, G. G. Lindsey and H. H. Klump, *J. Mol. Biol.*, 1993, **230**, 1278–1290.  
70 Y. Chen, S. H. Lee and C. Mao, *Angew. Chem., Int. Ed.*, 2004, **43**(40), 5335–5338.  
71 M. Gellert, M. N. Lipsett and D. R. Davies, *Proc. Natl. Acad. Sci. U. S. A.*, 1962, **48**, 2013–2018.  
72 Y. Oka and C. A. Thomas, Jr., *Nucleic Acids Res.*, 1987, **15**(21), 8877–8898.  
73 W. B. Sherman and N. C. Seeman, *Nano Lett.*, 2004, **4**(7), 1203–1207.  
74 A. Siddiqui-Jain, C. L. Grand, D. J. Bearss and L. H. Hurley, *Proc. Natl. Acad. Sci. U. S. A.*, 2002, **99**(18), 11593–11598.  
75 N. Makita, S. Inoue, T. Akaike and A. Maruyama, *Nucleic Acids Symp. Ser.*, 2004, **48**, 173–174.